

A Self-balanced, Liquid Resistive, High Impedance HV Divider

M. Denicolai* and J. Hällström¹

¹Helsinki University of Technology, Power Systems and High Voltage Engineering, PL 3000, 02015 TKK, Finland

*E-mail: marco.denicolai@iki.fi

Abstract: The measurement of transients of several hundreds of kilovolts poses considerable problems when the measured source is sensitive to loading. Traditional capacitive dividers can shift the resonance frequency of the measured device, giving a completely distorted view of the original waveform. The low impedance of a resistive divider, while providing a fast response time, can attenuate the voltage to be measured by more than its dividing ratio. This paper presents a liquid resistive, high impedance, high voltage divider designed to be self-balanced when positioned in proximity of a Tesla transformer. The divider liquid column is graded so that its resistance distribution matches the distribution of the surrounding electric field. Deconvolution is used to take into account the non-ideal frequency response of the divider and correct the measured waveforms accordingly. The impedance achieved is of the order of one megaohm, with a dividing ratio of 1:140000. The divider design technique can be used in applications where the field distribution is known.

Key Words: Liquid resistive; High voltage divider; Broadband divider; Tesla transformer; Deconvolution

INTRODUCTION

The measurement of pulsed voltages in the 100 kV to 1 MV range can usually be handled by traditional capacitive or resistive dividers as long as the voltage source being measured has relatively low output impedance. On the contrary, if the measured device is sensitive to resistive and capacitive loading, the divider insertion error is not negligible and measurements become problematic. Resistive dividers typically feature loading resistances of 1 to 50 kΩ for pulsed voltages and higher resistive values are suitable only for measurement of DC voltages. Capacitive dividers are usually bound to AC application at a 50/60 Hz frequency and exhibit minimum capacitances of some hundreds of picofarads. Universal dividers feature negligible resistive loading but their capacitance is as high as in plain capacitive dividers. Non-intrusive voltage meters (field mills, capacitive pickups, etc.) impose no loading on the measured device but require the contribution of conduction current to be taken into account and separated from the displacement current. This typically translates into serious bandwidth limitations, screening constraints or the need for recalibration after each change of the setup geometry^[1,2]. Tesla transformers feature output impedances in the range of some hundreds of kilohms and their resonance frequencies are influenced by their output capacitance. The reliable measurement of their output voltage requires

the load resistance to be in the order of one megaohm or higher. The load capacitance has to be below about 10 pF. Flashover distances are easily several meters, imposing also serious positional problems when designing a measuring system.

A liquid resistive divider is selected for the measurement as its construction is relatively simple and it allows for high ohmic values. The balancing of the resistance and shunt capacitance of each of its sections can be achieved by geometric symmetry. The frequency response of such a high impedance resistive divider is limited by its stray capacitances to the high voltage and ground terminals. This problem is usually alleviated by field control, using electrode geometries chosen to make the electric field density almost constant along the resistor. The solution adopted in this paper is to minimize the stray capacitances by modifying the divider geometry in order to follow the original electric field distribution. If the insertion of the divider doesn't perturb the original field distribution, displacement currents originating from the divider are eliminated.

This paper describes the divider geometry design process and its construction. The frequency response of the built divider is estimated by measuring its step response. A series of measurements is performed with a Tesla transformer^[3] and deconvolution in the frequency domain is used to reconstruct the actual waveforms from the measured ones. Finally, results achieved are discussed and conclusions are drawn.

DIVIDER DESIGN

Dimensional design

The Tesla transformer used for the measurements is made of a base structure, a 1.8 m long secondary winding, and a top toroid with an outer diameter of 1.5 m (see Fig. 1). An intentional bump in the toroid directs the originated discharges radially and almost horizontally. The maximum produced voltage is about 500 kV peak and discharges up to 3 m long have been measured. Required flashover clearances of at least 2.5 m, together with a minimal isotropic capacitance, limit the viable locations of the divider ground electrode and, therefore, influence its mechanical structure and dimensions. The safest location for the divider is on the top of the transformer, as that area is seldom perturbed by the long random discharges.

The divider is composed of a 2.7 m long multisection acrylic tube with a top toroid. The tube base features a copper cap that makes contact with the Tesla transformer's toroid. The divider's top toroid is grounded

by a horizontal connection to the wall. The tube is filled with a liquid resistive solution and an intermediate tap is arranged near its top, therefore providing the desired dividing ratio. Deionized tap water is used as the resistive solution.

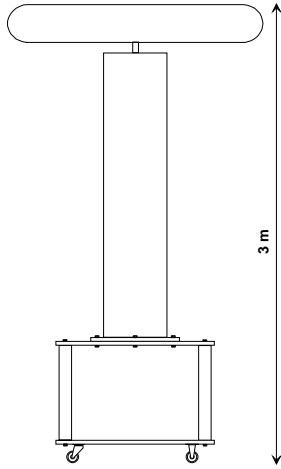


Fig. 1. The Tesla transformer to be measured with the aid of the designed divider.

The measurement setup is shown in Fig. 2. The divider is hanging from the ceiling and its position is upside down compared with the traditional location of column dividers, which is sitting on the floor. The function of the divider toroid is to enforce an electrical field with only vertical vector components between itself and the transformer toroid. A FEM solver package^[4] has been used to evaluate different diameters for the divider toroid. An outer diameter of 1.3 m was regarded as a good compromise.

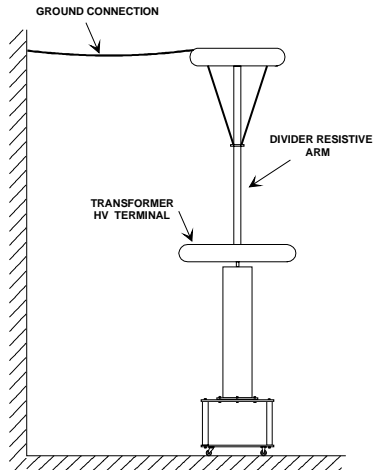


Fig. 2. Simplified measurement setup.

A sufficient requirement ensuring a fast response time and, therefore, a high bandwidth is that the electrostatic field distribution must approach the one inside the resistive element of the divider^[5]. Traditional field grading attempts to linearize the electrostatic field according to the linear resistive characteristic of the divider arm. In this work, instead, the resistive profile of the divider is modified in order to follow the distribution of the electrostatic field. The profile is changed by

building the acrylic tube using many sections with different lengths and inner diameters. Using the same FEM solver package the electrostatic field distribution was calculated with the probe tube first filled with air and then with water. The number, length, and diameter of the tube sections was empirically changed and the calculation was repeated until a satisfactory result was reached.

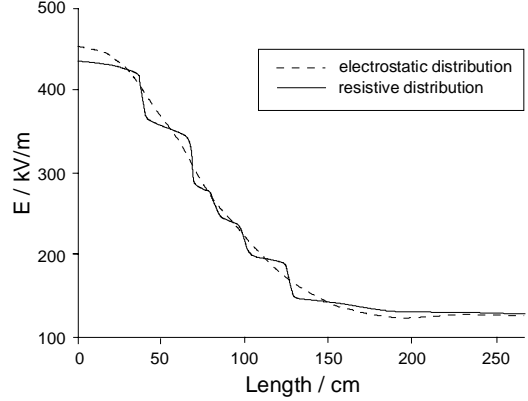


Fig. 3. Electrostatic vs resistive distribution of the electric field along the divider resistive arm longitudinal axis.

The solution shown in Fig. 3 was reached by using six different tube sections as listed in Table 1. Higher field densities required smaller inner diameters. Three extra PVC rods extending from the divider arm middle up to its toroid were added in order to stiffen the structure. Several acrylic collars were also glued across section boundaries for the same reason. The FEM solver estimated that the divider introduction accounted for a Tesla transformer toroid loading of 0.76 pF.

Table 1. Divider arm section sizes.

N.	Inner diameter [mm]	Length [mm]
1 (top)	80	1470
2	70	270
3	64	170
4	60	150
5	54	290
6 (bottom)	50	400

The top cap is made of solid copper and functions as the ground electrode. It uses a panel BNC female connector to provide contact with the divider tap (a copper disc) and also to set its distance from the cap (see Fig. 4). As each material boundary had to be sealed with epoxy glue, the minimum distance that could be achieved from the tap to the cap was 5 mm. The cap features two venting pipes and allows for residuals of gas dissolved in the divider filling solution to collect into its collar, yet ensuring complete immersion of the ground and tap plates.

Division ratio setup

The geometric symmetry of the divider structure should ensure the balancing of the resistance R_i and the capacitance C_i each of its N sections, that is

$$R_i C_i = k \quad i = 1..N \quad (1)$$

Changes of the sections' diameter (inner area S_i) or length l_i should not affect the divider balancing as

$$R_i \propto \frac{l_i}{S_i}, C_i \propto \frac{S_i}{l_i} \quad i = 1..N \quad (2)$$

This is no longer true after the ideal tap plate is replaced with the actual top cap assembly and the resistive column is placed between the transformer toroid and the divider's top toroid.

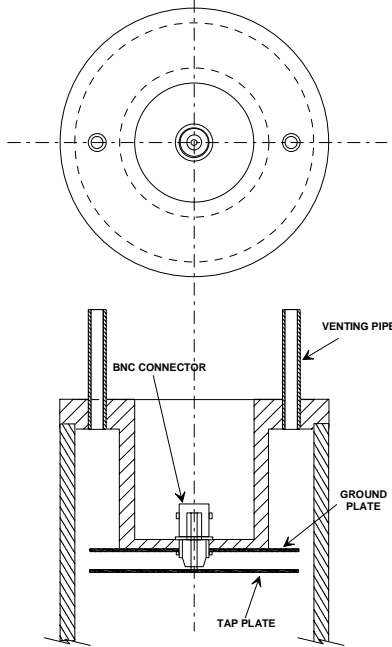


Fig. 4. The divider upper cap (section).

The FEM solver was used to estimate the capacitance C_I between tap and ground (top) electrodes. The tap potential was set to 1 V while both toroids were set to zero potential. The resulting potential distribution is shown in Fig. 5. The solver returned $C_I = 684$ pF, which is sensibly different from the original $C_I' = 548$ pF obtained with a simplified cap structure and without the top toroid.

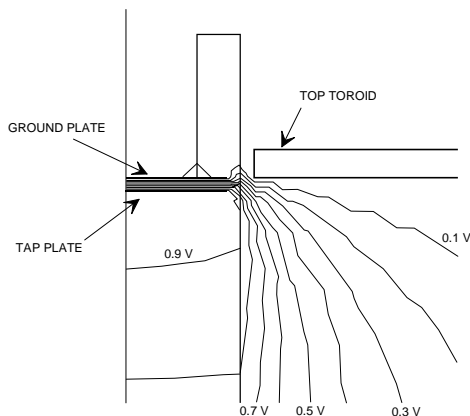


Fig. 5. Equipotential lines in the vicinity of the divider tap plate when its potential is set to 1 V.

This discrepancy translates into the need to externally compensate the lower arm of the divider. The divider was carefully assembled, cleaned and filled with deionized tap water. The AC resistance (at 50 Hz) measured

between the ground (top) and HV (bottom) electrodes was 1.618 M Ω and between ground and tap plates 2.32 k Ω . The divider was equipped with a battery powered broadband current buffer driving a 50 ohm impedance coaxial cable. The Tesla transformer toroid was disconnected from the secondary winding and driven by a 250 V step generator. The best response time was achieved after compensating the lower arm with a 1.7 k Ω resistance in parallel. As the resulting dividing ratio

$$r_i = \frac{1618000}{\frac{1}{\frac{1}{2320} + \frac{1}{1744}}} = 1625 \quad (3)$$

was not sufficient for handling a 500 kV input, a coaxial passive attenuator was added between the divider and the current buffer. The passive attenuator is built with non-inductive carbon resistors, has got an input impedance of 1.744 k Ω , and an attenuation ratio of 1:98. With the additional attenuator installed the calculated divider overall ratio is

$$r_d = r_i \cdot 98 = 1625 \cdot 98 = 159.3 \cdot 10^3 \quad (4)$$

CHARACTERIZATION OF THE DIVIDER

Estimation of the frequency response

The divider transfer characteristic is described in a comprehensive way by its frequency response. Under the assumption that the divider and its related hardware constitute a linear, causal and time-shift invariant system, the frequency response can be estimated from the measurement of its response to a step input^[6,7].

A mercury wetted relay was used to create a step function from c. 250 V to 0 V. The approximate fall time of the step is c. 1 ns. The step generator was positioned on the ground next to the base of the Tesla transformer, and a 390 Ω resistor was used to damp the oscillations due to the LC circuit created by the stray capacitance of the toroid and the inductance of the ground loop.

The waveform shown in Fig. 6 was measured after replacing the attenuator with a simple 1.744 k Ω resistor and applying a 250 V step. Noise removal was performed by averaging 200 acquisitions. The measured fall time was c. 40 ns. The ringing of the response tail is due to the resonant circuit formed by the stray capacitances of the transformer toroid to its secondary coil and of the coil to ground. This could be easily verified by grounding the secondary coil top and observing a corresponding frequency shift of the ringing.

An ideal step response was calculated, with initial and final levels found by averaging, respectively, the initial values and the tail values of the measured step. A ramp extending linearly from the first to the last sampled value was subtracted from both responses, in order to achieve two periodic waveforms. A Fast Fourier Transform (FFT) was computed for the responses and the divider frequency response was found by dividing the measured waveform FFT by the FFT of the ideal one.

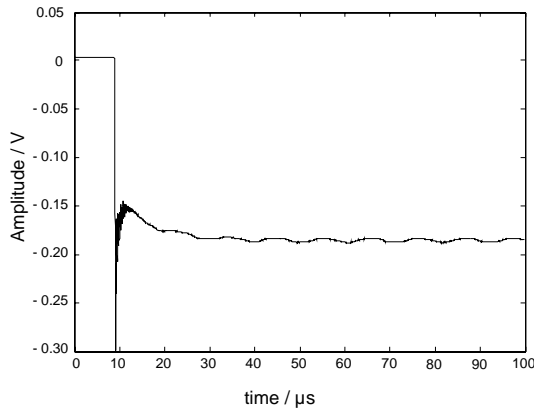


Fig. 6. Divider original step response, averaged and without further postprocessing.

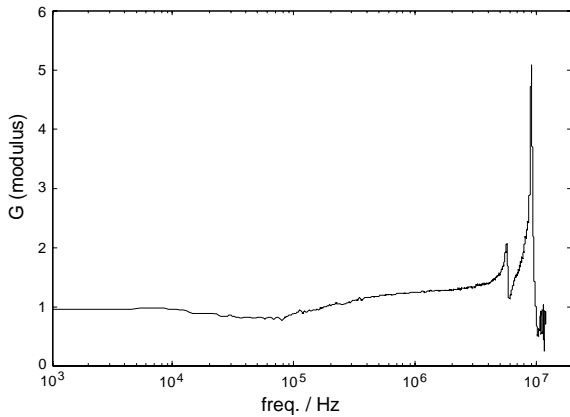


Fig. 7. Divider overall frequency response.

As during normal operation the Tesla transformer acts as a voltage source through its toroid, the resonances peaks due to the secondary coil proximity must be removed from the calculated divider frequency response. Linear interpolation is therefore used between 83 and 110 kHz, and between 227 and 250 kHz.

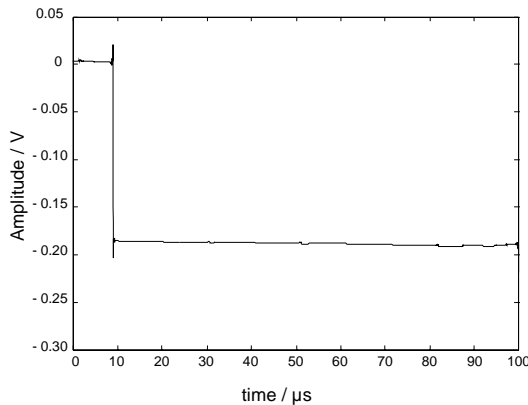


Fig. 8. Estimation of the ideal step response, obtained by deconvolution from the measured one in Fig. 6.

The resulting characteristic is shown in Fig. 7, deliberately truncated to 12 MHz in order to account for the measurement noise margin. The coaxial divider has been characterized for having a flat response in the 0 to 12 MHz band, therefore Fig. 7 represents the overall frequency response of the divider.

Deconvolution algorithm

Knowing the frequency response of the divider, deconvolution can be used to postprocess the acquired data and compensate for the distortion introduced by the non-ideal divider characteristic^[8]. The reconstruction algorithm developed within this work accepts as input an acquired sample sequence. Using the overlap-add method, the sequence is sliced into overlapping intervals that are deconvolved in the frequency domain with the probe frequency response and added back together in the time domain. Differences between sample rates are taken into account by using interpolation and decimation. The resulting signal is also passed through a low-pass filter with a cut-off frequency of 12 MHz.

Fig. 8 shows the ideal step reconstructed by deconvolving the measured waveform from Fig. 6 with the divider frequency response. Note that for this test the resonances caused by the secondary coil were not removed from the frequency response.

EXPERIMENTS AND RESULTS

The built divider has been tested by removing the coaxial attenuator and applying a standard 1/50 μs surge pulse with a peak value of 3780 ± 10 V. The surge generator was located on the floor next to the base of the Tesla transformer, and again a 390 Ω resistor was used to damp the loop oscillation. Fig. 9 shows the applied pulse measured with a reference capacitive divider.

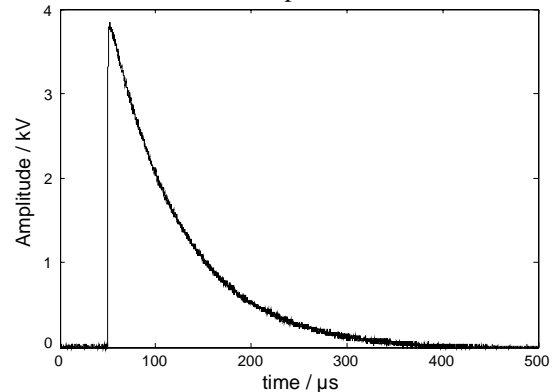


Fig. 9. Test surge pulse as measured with a calibrated reference divider.

The waveform acquired from the tested divider is shown in Fig. 10. Note how the transformer secondary coil resonance introduces the same kind of ripple already noticed with the step response in Fig. 6.

Fig. 11 shows the acquired pulse after deconvolution postprocessing: the benefits of the filtering are evident. The partial presence of the ripple in the filtered waveform is due to the slightly different measurement setup used for the surge test. The changed stray capacitance of the secondary coil causes a frequency shift of its ringing from the 96 kHz found during divider calibration to 92 kHz. During measurement of the Tesla transformer in operation this is not an issue as the coil acts as a voltage source.

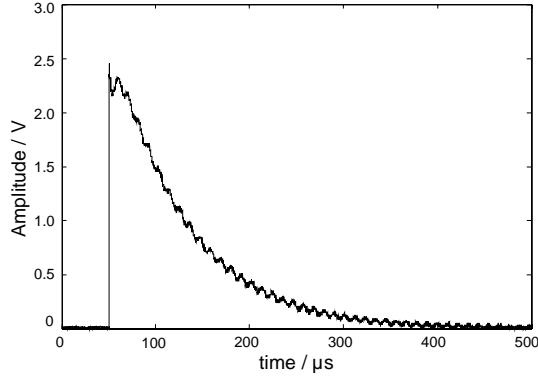


Fig. 10. Test surge pulse as measured with the built divider.

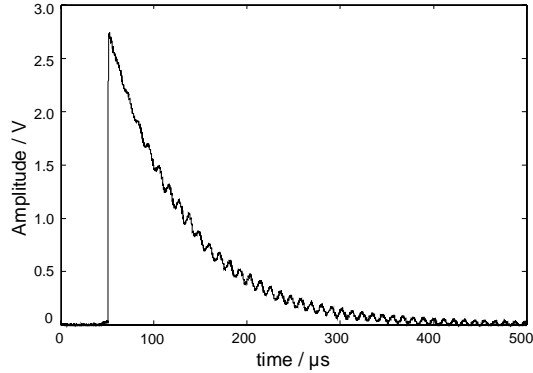


Fig. 11. Test surge pulse measured with the built divider after deconvolution postprocessing.

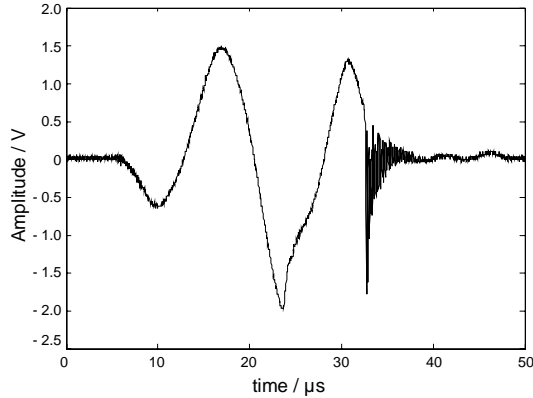


Fig. 12. Voltage burst measured from the Tesla transformer resulting in a discharge to a grounded target.

The divider ratio r'_t can be estimated by comparing the peak value measured by the reference divider V_{out} with the value V'_{out} measured by the built divider

$$r'_t = \frac{V'_{out}}{V_{out}} = \frac{3780}{2.735} = 1382 \quad (5)$$

The overall divider ratio with the coaxial attenuator installed is estimated as

$$r'_d = r'_t \cdot 98 = 1382 \cdot 98 = 135.4 \cdot 10^3 \quad (6)$$

The difference between the ratios r_t measured at 50 Hz and r'_t estimated with the surge pulse is due to the non-ideal frequency response of the divider and of its current buffer.

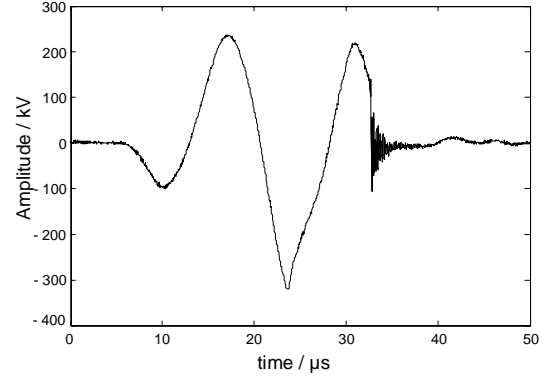


Fig. 13. The waveform from Fig. 12 corrected using the deconvolution algorithm to compensate for the non-ideal characteristics of the divider and multiplied by the divider ratio r'_d .

The built divider has also been used to measure the output voltage of the Tesla transformer in operation. As the transformer resonance frequency is as low as 66 kHz, the deconvolution algorithm doesn't introduce significant corrections to the measured waveforms. Slight differences can be noticed between Fig. 12 and Fig. 13 showing, respectively, a burst resulting in a breakdown to a grounded target and its corrected and scaled version. By increasing the Tesla transformer feed voltage, the divider has been tested up to a maximum peak potential of 418 kV.

CONCLUSIONS

(1) A high impedance liquid resistive divider with a 40 ns rise time and a ratio of 140000:1 has been designed and tested. The divider features a resistance of 1.6 MΩ and a capacitance of 0.76 pF (estimated). The design procedure of modifying the resistive column characteristic to follow the original electrostatic field gradient can be easily implemented using a FEM simulator. The approach is viable when the field distribution is known and can be assumed stable during the measurements.

(2) Deionized water has been successfully used together with copper electrodes. During a six months period no sedimentation, corrosion or resistance changes were noticed. It is worth mentioning that the divider was used to measure only AC and impulse voltages.

(3) The built divider can be easily characterized using its step response. With a sufficient sampling rate and data length, the extent of the calculated frequency response (in this work empirically fixed at 12 MHz) is only limited by the noise margin achieved during the measurement.

(4) The non-optimal step response of the divider, including even two resonances around 6 and 9 MHz, doesn't significantly affect its performance. Deconvolution in the frequency domain has been successfully used to compensate for the non-ideal transfer function of the divider and its current buffer. As expected, corrections are minimal for waveforms with only low frequency spectrum and more noticeable for fast edges.

(5) Future work needs to concentrate on justifying the source of the 6 and 9 MHz resonances, possibly due to the divider upper arm (the one between tap and HV electrode). An analysis of the divider uncertainty would also be useful.

ACKNOWLEDGEMENT

Special thanks to Paul Nicholson for his comments during the development of the divider and this manuscript.

REFERENCES

- [1] D. A. Rickard, J. Dupuy, R. T. Waters. Verification of an alternating current corona model for use as a current transmission line design. *IEE Proceedings-A*, vol. 138, no. 5, pp. 250-258, 1991.
- [2] P. E. Secker. The design of simple instruments for measurement of charge on insulating surfaces. *J. Electrostatics*, vol. 1, pp. 27-36, 1975.
- [3] M. Denicolai. Tesla Transformer for experimentation and research. Report TKK-SJT-52, High Voltage Institute, Helsinki University of Technology, 2001.
- [4] D. C. Meeker, BELA Electrostatics Solver, v 1.0, software available at <http://femm.foster-miller.com>
- [5] A. Di Napoli, C. Mazzetti. Electrostatic and electromagnetic field computation for the H.V. resistive divider design. *IEEE Trans. Power App. Syst.*, vol. PAS-98, no. 1, pp. 197-206, 1979.
- [6] R. H. McKnight, J. E. Lagnese, Y. X. Zhang. Characterizing transient measurements by use of the step response and the convolution integral. *IEEE Trans. Instrum. Meas.*, vol. 39, no. 2, pp. 346-352, 1990.
- [7] T. M. Souders, D. R. Flach. Accurate frequency response determinations from discrete step response data. *IEEE Trans. Instrum. Meas.*, vol. IM-36, no. 2, pp. 433-439, 1987.
- [8] H. Tang, A. Bergman. Uncertainty calculation for an impulse voltage divider characterized by step response. *ISH-II*, vol. 1, no. 467, pp. 62-65, 1999.